Egypt. J. Chem. **Vol. 65,** No. 10 pp. 657 - 665 (2022)

Egyptian Journal of Chemistry

http://ejchem.journals.ekb.eg/

Mechanical Properties and Wear Behavior of Polypropylene/Hydroxyapatite Nanocomposite

Nabeel Hasan Al-Mutairi[1]*, Massar Najim[1], Ohood Hmaizah Sabr[1], Fadhaa Atheer Kareem

[1]*Department of Polymer and Petrochemical Industries, College of Materials Engineering/University of Babylon, Iraq.*

Abstract

In this study, polypropylene (PP)/nano-hydroxyapatite (HA) nanocomposites were prepared using a twin-screw extruder to investigate the effect of different weight percentages of nano-HA (1, 2, and 3 wt.%) on the mechanical and tribological properties of PP. The tensile properties (i.e., tensile strength, modulus, and elongation at break) of the nanocomposites were determined; also, hardness, wear properties, and Fourier transform spectroscopy (FTIR), Scanning electron microscope (SEM), Differential scanning calorimetry (DSC) and contact angle (CA) were performed. The tensile test results showed that tensile strength and elongation increased to 23 MPa at 2% wt. of HA, while both Modulus and hardness increased with the increase in nano-HA content. By contrast, the wear rate and coefficient of friction (COF) decreased with the increase in nano-HA content. The FTIR results showed that only a physical interaction occurred between PP and nano-HA. SEM images indicate that there is a good dispersion of nano-HA within PP matrix. DSC results show that thermal stability improved with the addition of nanoHA.

Keywords: Polypropylene (PP); Hydroxyapatite (HA); nanocomposite; mechanical; wear properties; FTIR.

1. Introduction

The development of new materials that can mimic human tissue in order to reduce the risk of rejection by the human body is one of the most difficult challenges faced by modern medicine. According to a 2002 study conducted by the American Orthopedic Surgeons Association, bone implants are the second most frequent transplants after blood transfusions. In this context, researchers around the world have focused on developing new and improved hard tissue replacement implants with unique properties. They have been investigating the field of biomaterials for this purpose [1]–[3]. The bone is an important tissue/organ in the human body; it plays an important role in organizing muscles so they could perform various functions and could respond to environmental variations; moreover, it provides mechanical support, protects tissues, and is involved in hematopoiesis and mineral loading [4]–[7]. Metal components, such as stainless steel, chromium and cobalt, and titanium-based alloys, are used in the best orthopedic implants because of their excellent mechanical strength and ductility. However, their Young's modulus was far higher than that of human bones. This has a stress-relieving impact on the neighboring bone tissue, allowing it to sustain a greater portion of the implant's weight. The failure occurred as a result of the metal implant's resorption and disintegration. Furthermore, sodium chloride-containing human bodily fluids are hostile to metallic surfaces that are prone to corrode, causing the release of metallic ions that induce irritation, allergic reactions, and cytotoxicity [8]. Meanwhile, HA provides rigidity, and collagen fibrils provide flexibility and reinforcement to bones. Figure 1 shows how the biological building blocks of weight-bearing bones' dense outer sections are arranged for maximum structural support, as seen by the juxtaposed assembly of diverse structures with varying topologies, ranging from folded structures to larger super structural units [9].

The primary inorganic component of vertebrate hard tissues is hydroxyapatite (HA). An artificially synthesized HA is bioactive (osseoconductive), that is, it promotes bone development on its surface in the presence of viable bone or differentiated bone-forming cells [10]. Artificially synthesized HA ceramics (in porous, powder, and dense forms) have therefore been used in orthopedic and dentistry applications [11]–

*Corresponding author e-mail: nabeeleng90@gmail.com.; (Nabeel Hasan Al-Mutairi).
Receive Date: 15 December 2021, Revise Date: 07 February 2022, Accept Date: 24 February 2022
DOI: 10.21608/EJCHEM.2022.111440.5067

[13], whereas traditional HA ceramics are only used in non-load-bearing bones due to their poor mechanical characteristics.

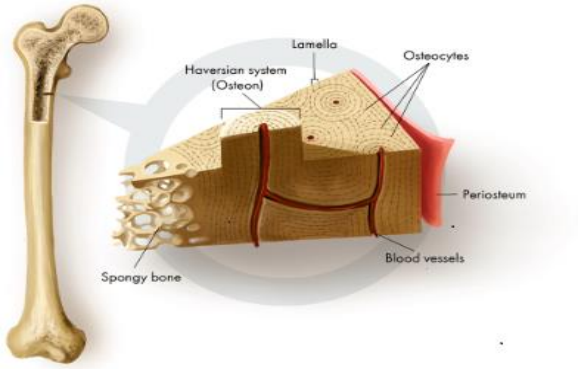

Figure 1: The distinct and intricate organization characterizing the internal bone structure.

Consequently, combining HA with other substances, such as polymer, has been becoming increasingly popular. Bonfield invented the bio-ceramics/polymer composite concept, wherein bone, which is an organic matrix, is reinforced with HA nanoparticles [14]. The addition of HA to bone cement might improve its biocompatibility as well as its mechanical properties [15]–[18]. The amount of added HA affects the thermal and mechanical characteristics of bone cement [19]. Moreover, it has been reported that surface properties and particle size affects the mechanical properties of bone cement [20], [21].

Polyolefin–HA composites ($Ca_{10}(PO_4)6(OH)_2$) have emerged as viable alternatives. Polymers are an appropriate use in the field of biomedicine because of their light weight, simplicity of production, and comparatively low cost. By reinforcing using micrometer-sized fillers, the tensile stress and modulus could be evaluated. As a result, the composite approach is a good way to make bone transplants out of polymers with good mechanical characteristics [22], [23]. The development of novel materials for the replacement and repair of natural bones has considerably sparked attention in recent years [24]. Biocompatible and biostable polypropylene (PP) can be used as a matrix material for bioactive composites instead of polyethylene (PE). Mechanical fatigue performance and mechanical property loss at high temperatures are both critical for bone replacement materials and PP outperforms PE in each of these areas. Any load-bearing implant must be capable of maintaining mechanical characteristics while withstanding millions of loading–unloading cycles at body temperature [24], [25].

A PP reinforced with HA (PP/HA) biocomposite has been created, and some aspects of this composite have been investigated. The manufacture, structure, and mechanical properties of PP/HA composites have been investigated using a systematic approach [24].

In this study, PP and different percentages (1%, 2%, and 3%) of nano-HA were prepared using a twin-screw extruder to be used as lightweight bone replacement. The effects of nano-HA on the mechanical, thermal, morphological and wear properties of PP were studied.

2. Materials and Experimental Procedures

2.1. Materials and Methods

HA nanopowder with a particle size 20 nm was obtained from N&R INDUSTRIES, INC. Different weight percentages of HA nanopowder (1, 2, and 3 wt.%; Table 1) were dispersed in acetone for 15 min using an ultrasonication device and then mixed manually with PP pellets. Subsequently, the PP pellets mixed with nano-HA dried in an oven at 70°C for 30 min. The mixture was then placed in a twin-screw extruder at 130°C and 150°C for zones 1 and 2, respectively, to obtain a composite sheet from PP and HA.

Table (1): The Composition of PP/HA Nanocomposite Materials.

Samples	(PP) wt.%	(HA) wt.%
PP	100	0
PP /1%-nanoHA	99	1
PP/2%-nanoHA	98	2
PP /3%-nanoHA	97	3

2.2. Characterization

The tensile strength of all samples was tested at a load of 5 KN and at a speed of 2 mm/min at room temperature. The prepared samples were cut according to ASTM D1708-02 for the determination of tensile strength, elongation at break, and elastic modulus. A Shore D hardness device was used to measure the hardness of the samples that were cut according to ASTM D 2240; the average of three readings was calculated to obtain accurate results for each sample.

Wear and friction tests were performed according to ASTM G99–05 by using a pin-on-disc machine. The dimensions of the tested sample (d*t) were 40 mm x 2mm, and it was sliding against a steel pin with a diameter of 6 mm; the sphere had a hardness of HRC 56, and a surface roughness of R = 3.2 μm in the vertical configuration. The pin slides in a track with a

diameter of 24 mm at a speed of 0.4 m/s, a sliding distance of 1000 m, and a load of 40 N.

The wear rate as a function of volume loss in cubic millimeters was calculated using equation (1) shown below [26]:

Volume loss= (ΔW/ρ) *1000 …… (1)

Where Volume loss: The volume of wear rate in mm^3, Δw: loss in sample weight before and after test (g), and ρ: density of spample (g/cm_3).

The interaction between PP and nano-HA and the shifting of bands were investigated using Fourier transformation spectroscopy (FTIR) type IR Affinity-1, the samples were examined at a wavelength of 500–4000 cm^{-1}.

Scanning electron microscope (SEM) has been used to identify the distribution of HA nanoparticles within PP matrix, also the compatibility of HA particles with PP.

Differential scanning calorimetry (DSC) has been used to evaluate thermal properties (T_m, T_c, ΔH, and X_c) of PP and its nanocomposites. The samples were heated from 25-250 °C, then cooled from 250-25 °C with a heating and cooling rate 10 °C/min.

The wettability of PP and its nanocomposites with HA at different wt. % percentages have been investigated using contact angle CA type SL 200C Static Contact Angle Meter, which using circle fitting method of water on samples surface.

3. Results and Discussion

3.1. Tensile test

The effects of the incorporating of HA nanopowder into PP on the tensile strength and the elongation at break of the nanocomposite at different percentages are shown in Figures 2 and 3. The tensile strength and elongation decreased with increased HA content; the tensile strength decreased from 22 MPa for pure PP to 17 MPa and 16 MPa at 1 wt.% and 3 wt.% HA, respectively. This result is due to the agglomeration of nanoHA that formed in the voids between the matrix PP and the filler particles HA. Furthermore, increasing the agglomeration of the dispersed filler particles reduced tensile strength, and the inclusion of the HA bioceramic stiffened the PP/HA nanocomposite, thus reducing both the tensile strength and the elongation at break. This result agrees with Liu and Wang [24]. While, at 2 wt.% HA, the highest tensile strength and elongation are 23 MPa and 385%, respectively, which can be attributed to the well-distributed particles within the matrix PP, which lengthen the crack propagation channel, absorb a portion of the energy, and promote plastic deformation. As a result, the strength of the nanocomposite increased.

Figure 4 shows the elastic modulus of the PP/HA nanocomposites. It can be seen that the elastic modulus increases as the HA content increases. The elastic modulus increased from 0.12 GPa for PP to 0.22 GPa for 3% wt. of HA, indicating that the addition of the HA bioceramic stiffened the PP/HA nanocomposites, which is consistent with the theories and general observations that fillers with a higher stiffness than the matrix can increase the elastic modulus of composites. Aside from the bioactivity brought about by the presence of HA, the greater Young's modulus and hardness of the PP/HA composite makes it ideal for hard tissue replacement [24], [27].

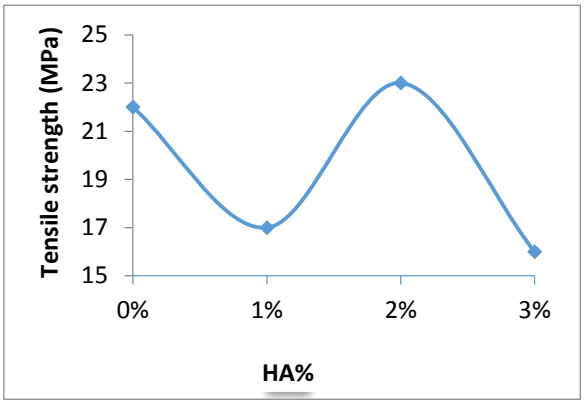

Figure 2: The tensile strength of PP as functions of weight percent of HA.

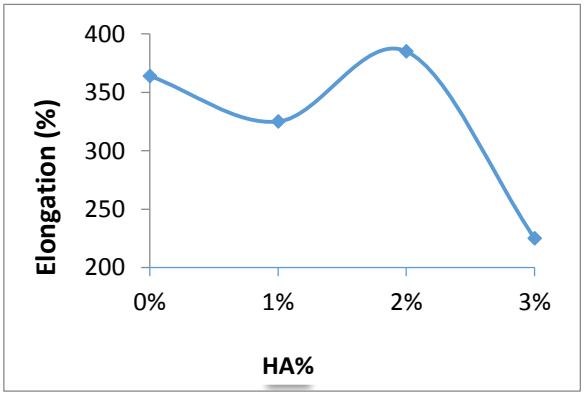

Figure 3: Elongation at break of PP as functions of weight percent of HA.

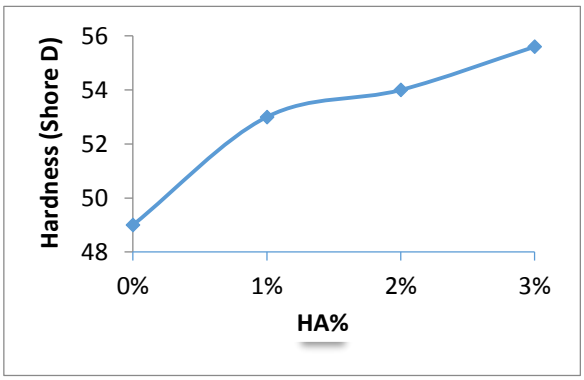

Figure 4: Elastic modulus of PP as functions of weight percent of HA.

3.2. Hardness result

Figure 5 shows that the Shore D hardness of the PP nanocomposites increased with the increase in nano-HA content. The hardness increased from 49 shore D for PP to 55.6 shore D for 3% wt. of nano-HA. This is because nano-HA is stiffer than the polymer and restricts the motion of molecular chains, resulting in higher resistance to penetration and hardness [28].

Figure 5: The Hardness of PP as functions of weight percent of HA.

3.3. Volumetric wear rate and coefficient of friction

Pin-on-disk device has been used to determine the effect of nano-HA addition with different weight fractions of HA (1 wt.%, 2 wt.%, and 3 wt.%) on the friction coefficient COF and volume loss, which were used to calculate the rate of friction. Figure 6 shows the effect of the different weight fractions of nano-HA on the wear rate, and Figure 7 illustrates the relationship between the wear rate and time. Its shown that there is a decrease in the volume loss of wear with an increase in nano-HA content. This is due to the efficient distribution of nano-HA in the PP matrix, as well as to the strong interaction between the polymer PP and the HA nanoparticles. The loss in volume decreased from 1.3 mm^3 for pure PP to 0.406 mm^3 at 3 wt.% of HA [29], [30].

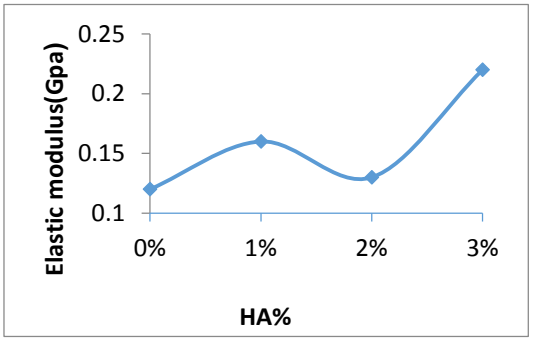

Figure 6: The Volume loss of PP/HA nanocomposite.

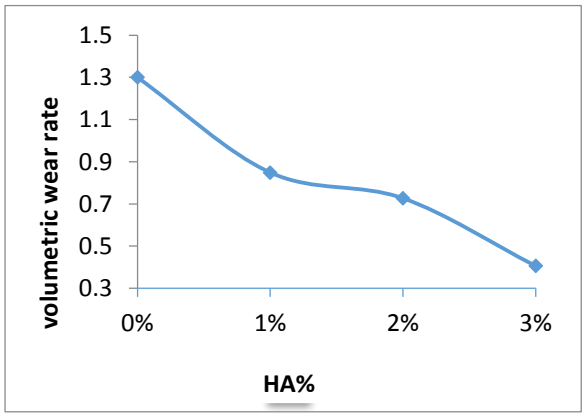

Figure 7: The relationship between wear rate and time as a function of HA.

The coefficient of friction (COF) shown in Figure 8 decreased with the increase of nano-HA content, the COF decreased from 0.47 for pure PP to 0.34 for 3 % wt. of HA, as shown in Table 2. This result can be attributed to the favorable interaction and homogenous dispersion between the polymer PP and HA nanoparticles, allowing for efficient load transfer from the PP matrix to the reinforcement HA nanoparticles. The COF also decreased due to the transfer of material from the composite to the hard metal counterface and the formation of a protective film. This film protects the nanocomposite materials from the hard pins, thus decreasing the COF and wear rate[30], [31].

Table (2): Coefficient of friction for PP and PP/HA nanocomposite.

Samples	Coefficient of friction (COF)
PP	0.47
PP /1%-nanoHA	0.40
PP/2%-nanoHA	0.41
PP /3%-nanoHA	0.34

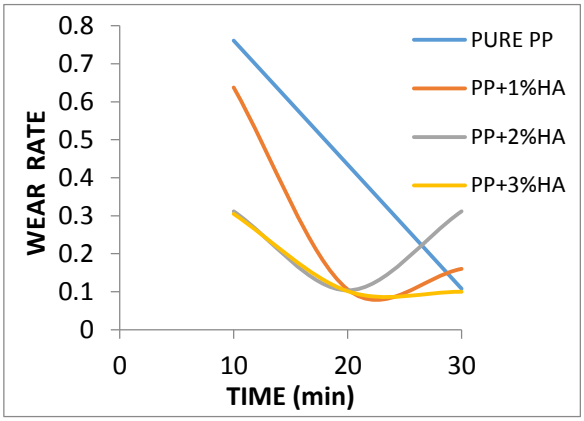

Figure 8: The coefficient of friction for pure PP and PP/HA nanocomposite.

3.4. FTIR Analysis

FTIR spectrometry was used to analyze the effect of the reinforcement material (nano-HA) on the chemical structure of the polymer (PP). Figure 9 shows the band values and the changes in these values with the addition of HA. Table 3 lists the most important bands of pure PP and its nanocomposites, as derived from Figure 9, and compares them with the bands mentioned in [32]. The following bands were identified for pure PP: 808.17 cm^{-1} for C–C stretching, 840.96 cm^{-1} for C–H rocking. The bands at 972.12 cm^{-}

[1] and 997.20 cm^{-1} for CH_3 rocking and C–C stretching, 1166.93 cm^{-1} for C–H wagging and CH^3 rocking, 1369.46 cm^{-1} and 1452.40 cm^{-1} for CH_3 symmetrical bending, 2868.15 cm^{-1} and 2914.22 cm^{-1} for CH_3 stretching and CH_2 asymmetrical stretching, and 2953.02 cm^{-1} for CH_3 asymmetrical stretching. The addition of nano-HA had no effect on the bands of pure PP, except for the CH_3 symmetrical bending bands shifting to 1369.82 cm^{-1} and 1454.33 cm^{-1} and the CH_3 asymmetrical stretching band shifting to 2949.16 cm^{-1}.From the results, it can be concluded that the interaction between the polymer PP and nano-HA is physical and not chemical.

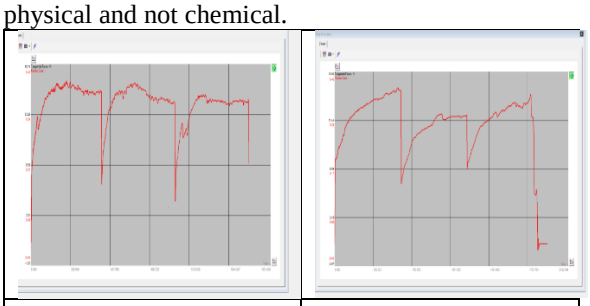

Pure PP | PP+1%HA

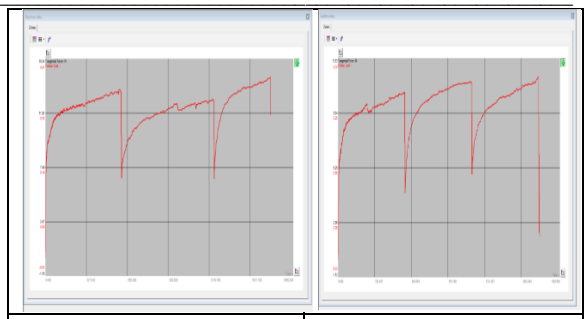

PP+2%HA | PP+3%HA

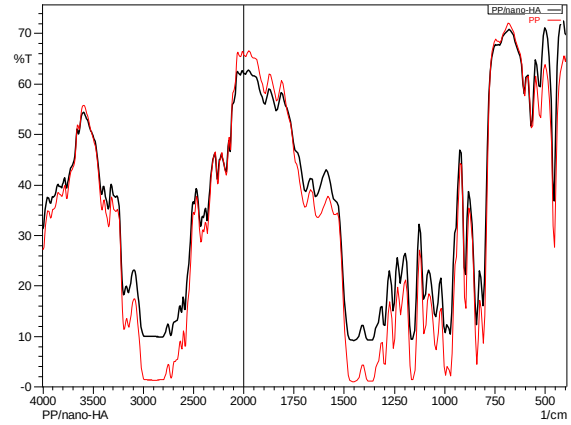

Figure 9: FTIR of PP and its nanocomposite with HA.

Table (3) The Transmission Bands of IR Spectrum for pure PP and PP/HA nanocomposite.

Type of bond	**PP standard** [32]	**Neat PP**	**PP+3% HA**
C-C stretching	808	808.17	808.17
C-H rocking	840	840.96	840.96
CH_3 rocking **C-C stretching**	973	972.12	972.12
CH_3 rocking **C-C stretching**	996	997.20	997.20
C-H wagging **CH_3 rocking**	1166	1166.93	1166.93
CH_3 symmetrical bending	1376 1456	1369.46 1452.40	1369.82 1454.33
CH_3 stretching	2870	2868.15	2868.15
CH_2 asymmetrical stretching	2920	2914.44	2914.44
CH_3 asymmetrical stretching	2950	2953.02	2949.16

3.5. SEM Images results

Figure 10 shows the SEM images of nanocomosites at different scales (10, 5, and 2) µm. The images for all percentages shows a good dispersion of nano-HA within the PP matrix and also a good interfacial bonding between the reinforcement nano-HA and matrix PP, that reflected on the some properties (mechanical and wettability) of PP/HA nanocomposites [33]. Also, it's shown that the absence of voids and defects on the nanocomposites (PP/HA) surface as in the literature of Chan et.al [8].

3.6. DSC result analysis

The thermal behavior of PP and its nanocomposites with different percentages of HA have been studied using DSC device as indicated by Figure 11. Figure 11a shows the melting temperature (T_m) of PP and PP/nano-HA, its shown that the melting temperature increased with the increase of HA nanoparticles. The melting temperature increased from 163.39 °C for PP to 165.18 °C, 165 °C, and 164.79 °C for 1%, 2%, and 3% of nano-HA respectively. This enhancement due to the good thermal properties of HA as in the literature of shao-Zhi [34]. Also, from Figure 11b, its shown that the crystallization temperature (T_c) have been slightly improved, this improvement may attribute to the good dispersion of nanoparticles HA within PP matrix. All the data that observed from DSC are tabulated in Table 4. Also, its found that the degree crystallinity of nanocomposites PP/HA decreased at 1% and 3% of nano-HA, while increased at 2% of

nano-HA due to the better compatibility and dispersion at this percentage, these results are so correlated with the tensile strength results [35]. From the results above, it can concluded that the thermal stability of nanocomposites PP/HA have been improved by the addition of nanoHA.

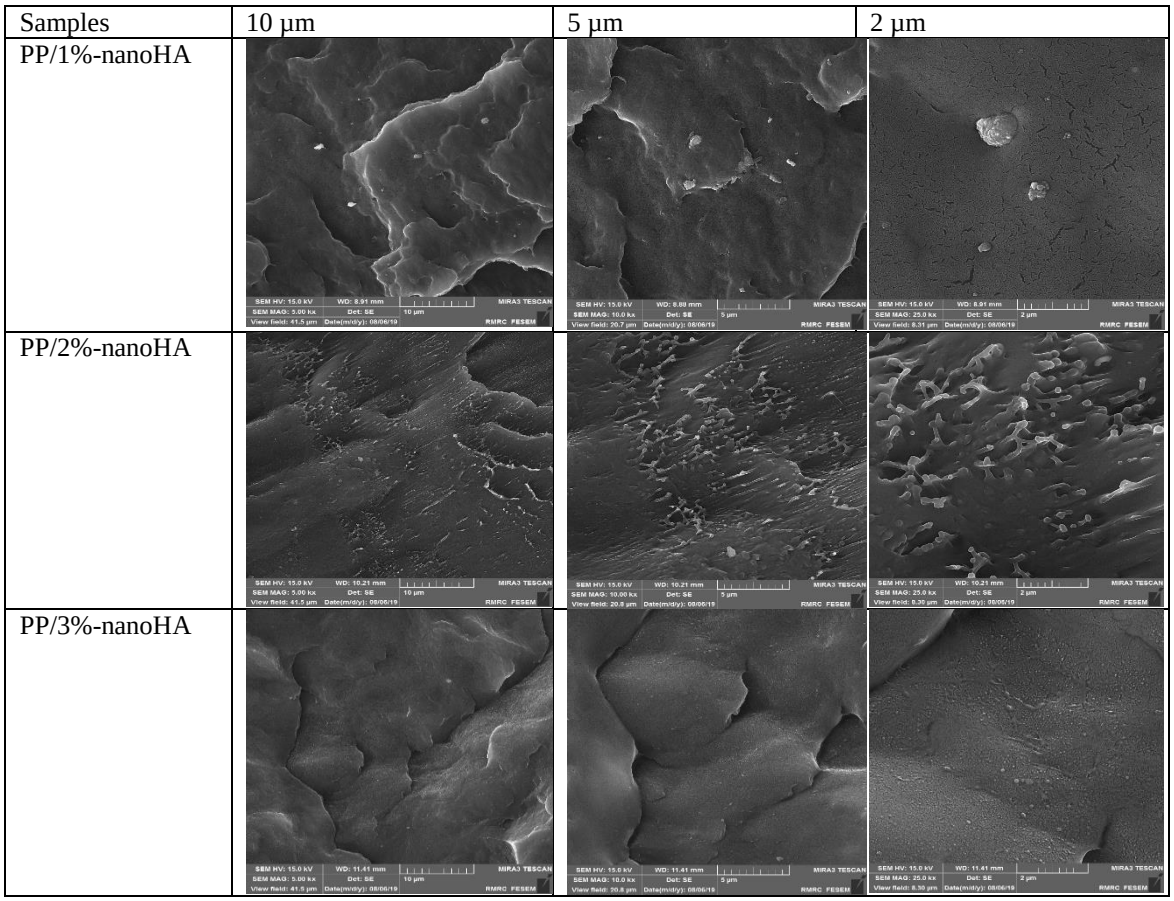

Figure 10: SEM images of PP/HA nanocomposites.

Table 4: The thermal properties of PP and PP/HA obtained from DSC.

Samples	T_m (°C)	T_c (°C)	ΔH_m (J/g)	X_c %
PP	163.39	111.31	107.1	51.24
PP/1%-nanoHA	165.18	111.33	94.89	45
PP/2%-nanoHA	165	111.62	132.16	62
PP/3%-nanoHA	164.79	111.46	103.12	47.9

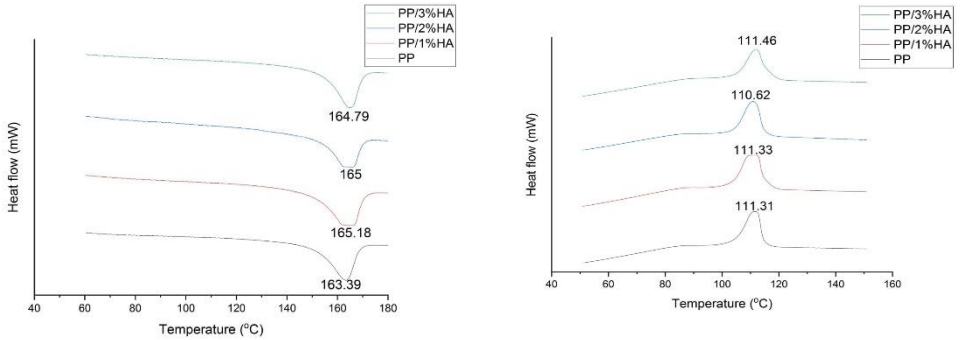

Figure 11: DSC thermograms for PP and PP/nano-HA, a) Heating, b) Cooling.

3.7. Contact angle CA results

Table 4 shows the CA of PP and its nanocomposites with nano-HA particles at 0 and 60 sec. As shown by Table 5, the contact angle decreased with the increase of nano-HA content, which mean that the surface of PP become more able to be wet (more hydrophilic) as indicated by SEM images. The more hydrophilicity, means that the adhesion between the bone (PP/HA nanocomposites) and the tissues that will generated around the bone (PP/HA nanocomposites) are more favorable [36].

Table 5: Contact angle CA Data for PP and PP/HA nanocomposites.

Materials	Contact Angle	Time
PP	86º	0 sec
	76.5º	60 sec
PP/1%-nanoHA	82.1º	0 sec
	78.5º	60 sec
PP /2%-nanoHA	82.1º	0 sec
	75.4º	60 sec
PP/3%-nanoHA	77.9º	0 sec
	75.1º	60 sec

4. Conclusion

Nanocomposites using PP and nano-HA particles were synthesized by twin-screw extruder to study the effects of nano-HA on the mechanical, thermal, morphological and wear properties of the resulting nanocomposites. The tensile strength and the elongation at break decreased at 1 wt. % and 3 wt. % HA, respectively, while increased at 2 wt. % HA. The hardness of the nanocomposite increased with increasing HA content due to the higher stiffness of nanopartcles, while both the wear rate and COF decreased with increasing HA content. FTIR spectrums of PP and PP/nano-HA shows that there is no change in wavenumber bands, which is an indication of the absence of chemical reaction between PP and nano-HA. SEM images shows that there is a good distribution and compability of nano-HA within PP matrix that reflected on wear properties and contact angle. DSC analysis results reveled an improvement in thermal stability of nanocomposites, the melting temperature T_m and crystallization temperature T_c have been enhanced by the addition of nanoHA, while the dgree of crystallinity X_c improved only at 2%-nanoHA.

5. References

[1] C. S. C. Sabrina Constanda, Miruna Silvia Stan, R. G. Mikael Motelica-Heino, and and D. P. Khalid Lafdi, Anca Dinischiotu, "Carbon nanotubes-hydroxyapatite nanocomposites for an improved osteoblast cell response," *J. Nanomater.*, vol. 2016, pp. 1–10, 2016.

[2] D. Lahiri, S. Ghosh, and A. Agarwal, "Carbon nanotube reinforced hydroxyapatite composite for orthopedic application: a review," *Mater. Sci. Eng. C*, vol. 32, no. 7, pp. 1727–1758, 2012.

[3] O. Sabra, A. Husseina, and M. Obaida, "Preparation and evalution water resistance, mechanical and morpholgical characteristics of PVA/SiO2 nanocomposites for food industry applications," *Dig. J. Nanomater. BIOSTRUCTURES*, vol. 16, no. 2, pp. 733–745, 2021.

[4] C. Gao, S. Peng, P. Feng, and C. Shuai, "Bone biomaterials and interactions with stem cells," *Bone Res.*, vol. 5, no. 1, pp. 1–33, 2017.

[5] H. Lu, Y. Liu, J. Guo, H. Wu, J. Wang, and G. Wu, "Biomaterials with antibacterial and osteoinductive properties to repair infected bone defects," *Int. J. Mol. Sci.*, vol. 17, no. 3, p. 334, 2016.

[6] A. V Maksimkin *et al.*, "Multilayer porous UHMWPE scaffolds for bone defects replacement," *Mater. Sci. Eng. C*, vol. 73, pp. 366–372, 2017.

[7] L. Terranova, R. Mallet, R. Perrot, and D. Chappard, "Polystyrene scaffolds based on microfibers as a bone substitute; development and in vitro study," *Acta Biomater.*, vol. 29, pp. 380–388, 2016.

[8] K. W. Chan, H. M. Wong, K. W. K. Yeung, and S. C. Tjong, "Polypropylene biocomposites with boron nitride and nanohydroxyapatite reinforcements," *Materials (Basel).*, vol. 8, no. 3, pp. 992–1008, 2015.

[9] B. Lowe, J. G. Hardy, and L. J. Walsh, "Optimizing nanohydroxyapatite nanocomposites for bone tissue engineering," *ACS omega*, vol. 5, no. 1, pp. 1–9, 2019.

[10] B. D. Ratner, A. S. Hoffman, F. J. Schoen, and J. E. Lemons, *Biomaterials science: an introduction to materials in medicine*. Elsevier, 2004.

[11] H. Aoki, "Medical applications of hydroxyapatite. Tokyo: Ishiyaku EuroAmerica." Inc, 1994.

[12] M. Jarcho, "Calcium phosphate ceramics as hard tissue prosthetics," *Clin. Orthop. Relat. Res.*, vol. 157, pp. 259–278, 1981.

[13] K. A. Hing, S. M. Best, K. E. Tanner, P. A. Revell, and W. Bonfield,

"Histomorphological and biomechanical characterization of calcium phosphates in the osseous environment," *Proc. Inst. Mech. Eng. Part H J. Eng. Med.*, vol. 212, no. 6, pp. 437–451, 1998.

[14] M. Okada and T. Matsumoto, "Fabrication methods of hydroxyapatite nanocomposites," *Nano Biomed.*, vol. 8, no. 1, pp. 15–26, 2016.

[15] E. J. H. and W. B. M. J. Dalby, L. Di Silvio, "Initial Interaction of Osteoblasts with the Surface of Hy-droxyapatite-Poly(Methylmethacrylate) Cement," *Biomaterials*, vol. 22, no. 13, pp. 1739–1747, 2001.

[16] M. J. Dalby, L. Di Silvio, E. J. Harper, and W. Bonfield, "Increasing hydroxyapatite incorporation into poly (methylmethacrylate) cement increases osteoblast adhesion and response," *Biomaterials*, vol. 23, no. 2, pp. 569–576, 2002.

[17] T. Saito, Y. Kin, and T. Koshino, "Osteogenic response of hydroxyapatite cement implanted into the femur of rats with experimentally induced osteoporosis," *Biomaterials*, vol. 23, no. 13, pp. 2711–2716, 2002.

[18] R. D. Welch *et al.*, "Subchondral defects in caprine femora augmented with in situ setting hydroxyapatite cement, polymethylmethacrylate, or autogenous bone graft: biomechanical and histomorphological analysis after two- years," *J. Orthop. Res.*, vol. 20, no. 3, pp. 464–472, 2002.

[19] K. ŞERBETÇİ, F. Korkusuz, and N. Hasirci, "Mechanical and thermal properties of hydroxyapatite-impregnated bone cement," *Turkish J. Med. Sci.*, vol. 30, no. 6, pp. 543–549, 2000.

[20] S. Y. Kwon, Y. S. Kim, Y. K. Woo, S. S. Kim, and J. B. Park, "Hydroxyapatite impregnated bone cement: in vitro and in vivo studies," *Biomed. Mater. Eng.*, vol. 7, no. 2, pp. 129–140, 1997.

[21] Z. SM, S. S A, S. T Ebrahimi, and S. S A, "A study on mechanical properties of PMMA/hydroxyapatite nanocomposite," *Engineering*, vol. 2011, 2011.

[22] R. Oréfice, A. Clark, J. West, A. Brennan, and L. Hench, "Processing, properties, and in vitro bioactivity of polysulfone- bioactive glass composites," *J. Biomed. Mater. Res. Part A*, vol. 80, no. 3, pp. 565–580, 2007.

[23] L. C. Du, Y. Z. Meng, S. J. Wang, and S. C. Tjong, "Synthesis and degradation behavior of poly (propylene carbonate) derived from carbon dioxide and propylene oxide," *J. Appl. Polym. Sci.*, vol. 92, no. 3, pp. 1840–1846, 2004.

[24] Y. Liu and M. Wang, "Manufacture and Characterisation of a Bone Analogue Biomaterial: Hydroxyapatite Reinforced Polypropylene," 2004.

[25] M. N. Obaid, O. H. Sabr, and A. A. Hussein, "Characteristic of polypropylene nanocomposite material reinforcement with hydroxyapatite for bone replacement," *J. Achiev. Mater. Manuf. Eng.*, vol. 104, no. 1, 2021.

[26] T. Ilchmann, M. Reimold, and W. Müller-Schauenburg, "Estimation of the wear volume after total hip replacement: a simple access to geometrical concepts," *Med. Eng. Phys.*, vol. 30, no. 3, pp. 373–379, 2008.

[27] J. Ni and M. Wang, "In vitro evaluation of hydroxyapatite reinforced polyhydroxybutyrate composite," *Mater. Sci. Eng. C*, vol. 20, no. 1–2, pp. 101–109, 2002.

[28] O. H. Sabr, N. H. Al-Mutairi, and A. Y. Layla, "Characteristic of low-density polyethylene reinforcement with nano/micro particles of carbon black: a comparative study," *Arch. Mater. Sci. Eng.*, vol. 2, no. 110, pp. 49–58, 2021, doi: 10.5604/01.3001.0015.4312.

[29] D. Berman, A. Erdemir, and A. V Sumant, "Reduced wear and friction enabled by graphene layers on sliding steel surfaces in dry nitrogen," *Carbon N. Y.*, vol. 59, pp. 167–175, 2013.

[30] N. A. Saad and M. N. Obaid, "The synergetic Effect of Short Fibers of PAN and Nanoparticles (GNP/HAp) on Tribological Behavior and Surface Roughness of UHMWPE," *Test Eng. Manag.*, vol. 83, pp. 22000–22012, 2020.

[31] M. N. Obaid and S. H. Radhi, "Enhancement of tribological properties and characteristic of polymer matrix composite (UHMWPE reinforced with short fibres of polyester) for Total Disc Replacement (TDR)," *J. Achiev. Mater. Manuf. Eng.*, vol. 102, no. 2, 2020.

[32] J. Fang, L. Zhang, D. Sutton, X. Wang, and T. Lin, "Needleless melt-electrospinning of polypropylene nanofibres," *J. Nanomater.*, vol. 2012, 2012.

[33] J. K. Oleiwi, R. A. Anaee, and S. A. H. Radhi, "Tensile Properties of UHMWPE Nanocomposites Reinforced by CNTs and nHA for Acetabular Cup in Hip Joint Replacement," *J. Eng. Appl. Sci.*, vol. 13, no. 13, 2018.

[34] Z. Fu, ShaoZhi Wang, XiuHong Guo, Gang Shi, Shuai Liang, Hang Luo, Feng Wei, YuQuan, Qian, "Preparation and

characterization of nano-hydroxyapatite/poly (ε-caprolactone)− poly (ethylene glycol)− poly (ε-caprolactone) composite fibers for tissue engineering," *J. Phys. Chem. C*, vol. 114, no. 43, pp. 18372–18378, 2010.

[35] Y. M. Xiang Zhang, Yubao Li, Guoyu Lv, Yi Zuo, "Thermal and crystallization studies of nano-hydroxyapatite reinforced polyamide 66 biocomposites," *Polym. Degrad. Stab.*, vol. 91, no. 5, pp. 1202–1207, 2006.

[36] A. A. Hussein and O. H. Sabr, "Preparation and facilitation of antibacterial activity, hydrophilicity of piezo-PVDF/n-MgO film by electro-spinning and spin coated for wound dressing: A comparative study," *J. Mech. Eng. Res. Dev*, vol. 42, no. 2, pp. 23–31, 2019.